Heat Release Rate and NOx Formation Process in Two-Stage Injection Diesel PCCI Combustion in a Constant-Volume Vessel

AUTHOR(S):

Horibe, Naoto; Annen, Takahisa; Miyazaki, Yuichi; Ishiyama, Takuji

2010-01-0608

Heat Release Rate and NOx Formation Process in Two-Stage Injection Diesel PCCI Combustion in a Constant-Volume Vessel

Naoto HORIBE, Takahisa ANNEN, Yuichi MIYAZAKI and Takuji ISHIYAMA
Graduate School of Energy Science, Kyoto University

ABSTRACT

The objective of the present study is to elucidate the combustion process of partial premixed charge compression ignition (PCCI) combustion using multiple injections in diesel engines. The effects of the ratio of the quantity of fuel used in the first and second injections, and the injection dwell time on heat release rate, soot and nitrogen oxide (NOx) formations are investigated in simulated partial PCCI combustion using a constant-volume vessel. N-heptane is used as fuel. The experiments are carried out under an ambient condition of 2 MPa and 900 K, which simulates a PCCI-like heat release rate with long ignition delays. The oxygen concentration is set to 21 and 15% to simulate conditions without and with exhaust-gas recirculation (EGR), respectively. The fuel quantity in the first injection is varied between 10 to 40% of the total fuel quantity, and the injection dwell is varied between 0.5 to 2.0 ms. Combustion analyses are carried out based on heat release rates and high-speed shadowgraph photographs. Image analyses of luminous flames are conducted to estimate soot formation and decay. NOx concentrations during combustion are measured using a total gas-sampling apparatus. The results show that, for the ordinary ambient oxygen mole fraction, longer injection dwells reduce the peak of the initial heat release rate in the case of a small amount of fuel used in the first injection; however, this effect is not found when a large amount of fuel is used in the first injection. By reducing the oxygen mole fraction, the above effect is obtained regardless of the quantity used for the first injection. An increase in the size of the first-injection quantity shortens the duration of the luminous flame. In a reduced ambient oxygen situation, the duration and area of the luminous flame increase as the injection dwell is longer. Regardless of the ambient oxygen mole fraction, the final NOx mass per released heat is reduced using two-stage injection, especially in the case of a long injection dwell.

INTRODUCTION

Combustion technologies based on homogeneous charge compression ignition (HCCI) combustion and PCCI combustion have been widely studied because they are expected to achieve significantly low NOx and particulate matter (PM) emissions under low-load conditions in diesel engines [1-4]. PCCI combustion was first attempted by means of a significantly early fuel injection, which provides a highly homogeneous, lean mixture due to the long ignition delay, realizing a simultaneous reduction of soot and NOx. However, the early-injection method dilutes the lubricating oil, increases unburned species emissions, and deteriorates thermal efficiency due to the difficulty of optimizing combustion phasing. Therefore, combustion strategies with moderately early fuel injection (≈20 deg BTDC) have been considered as more practical methods, and have been widely investigated [5-9], as they are advantageous in preventing the dilution of lubricating oil by fuel. In these strategies, very high EGR rates (higher than 50%) and lower compression ratios are essential to ensure sufficient fuel-air mixing time, suppression of NOx formation, and adequate combustion phasing.

However, the mixing time is much shorter compared to PCCI with a significantly early injection. As a result, except for the case of very small injection quantities, a small part of injected fuel burns in a mixing-controlled combustion mode, i.e., a diffusion combustion mode. Therefore, this combustion method is not pure PCCI, but partial PCCI combustion. In PCCI combustion with moderately early injection, optimization of the EGR rate, compression ratio and injection timing is effective in obtaining low soot and NOx emissions. On the other hand, a high pressure rise rate, which causes high combustion noise levels, is a challenging problem. Reduction of the pressure rise rate to a pilot-diesel level (<0.5 MPa/deg) is difficult because a large part of the injected fuel ignites within a small time difference after fully mixing with air. High-level emissions of hydrocarbon (HC) and carbon monoxide (CO) are also problems to be solved.

To solve these problems, partial PCCI combustion with multiple injections has been recently investigated [10-18]. Multiple stage diesel combustion (MULDIC) [11] employs a multi-injector system, in which half of the total fuel is injected at a very early timing (150 deg BTDC) by side injectors to generate a highly homogeneous mixture that burns in PCCI mode, while the remaining fuel is injected by a central injector to provide mixing-controlled combustion. In the early stage of the development of the combustion method, first-stage (PCCI mode) and second-stage (mixing-controlled or diffusion combustion mode) heat release processes were perfectly separated. This yielded low NOx and soot emissions; however, the thermal efficiency was lower than with ordinary diesel operation. Further research [12] indicated that merging first- and second-stage combustion and employing EGR provided high thermal efficiency. However, the problem of the high pressure rise rate remained.

Hardy and Reitz proposed Two-Stage Combustion (TSC) [13], which employed a similar combustion process to MULDIC, although only a single injector was used. The fuel injection parameters, intake boost pressure, and EGR were optimized based on experimental data using a merit function. Results showed that the trade-off between PM and NOx was significantly improved, without an excessive increase in HC emissions under medium loads. In a related study [14], Sun optimized the intake valve closure (IVC) timing, EGR ratio, start of late-injection timing, and fraction of fuel in HCCI combustion using computational fluid dynamics (CFD) simulation. The results showed that the TSC strategy was able to achieve very low engine-out emissions under medium-load operating conditions combining late IVC timing, late main injection timing, medium EGR levels, and a high fuel ratio in HCCI combustion. However, Sun noted that the peak pressure and pressure rise rate should be reduced within the physical constraints of the engine.

Weiskirch also proposed a similar combustion method, Split Combustion (SC) [15], although the first-stage injection was split into several parts. Experiments using this method were conducted under low- to high-load conditions. The results showed that the concept realized a remarkable reduction in NOx and soot emissions, along with a decrease in thermal efficiency of 10 to 30% compared to a conventional diesel strategy, and the emissions of HC and CO were reduced compared to PCCI combustion using early single-stage injection because the in-cylinder temperature was kept relatively high. In this case, the high pressure rise rate remained a challenging problem.

Koci performed experiments and simulations on the effects of two-stage injection in the Low Temperature Combustion (LTC) regime with a high EGR level [16]. Injection dwell was fixed, and the second injection was initiated around the time a small amount of heat is released by the cool flame of the first injection. The results indicate that two-stage injection is effective in reducing unburned HC, CO and PM emissions compared to single injection with “sweet-spot” injection timing [7], and retarding the injection timings close to TDC reduces combustion noise, while maintaining single injection emission levels. However, there is a trade-off between combustion noise and unburned species emissions, and sufficient reduction of combustion noise accompanies decreased thermal efficiency.

In a previous study [17], we examined the effect of two-stage injection with relatively small fuel quantities in first-stage injection (5–15 mm^3 in total quantities of 20–30 mm^3), moderately early first injection timing (5–25 deg BTDC), and a 25–55% EGR rate with a focus on the reductions of unburned species emissions and maximum pressure rise rate. Two-stage injection was advantageous in improving the trade-off between emissions and the pressure rise rate. However, smoke emission tends to increase compared to single injection and is sensitive to the selection of injection timings. Selecting conditions to provide low smoke emission tends to deteriorate thermal efficiency.

Thus partial PCCI combustion with two-stage injection is advantageous in improving emissions and combustion noise. However, the trade-offs between unburned species emissions and combustion noise, as well as between combustion noise and thermal efficiency are barriers for further improvement. The excessive sensitivity of smoke emission to the selection of injection conditions is also a problem. To fully utilize the multiple injection strategy, it is necessary to optimize not only ordinary parameters in single injection such as injection pressure and EGR rate, but also additional parameters such as timings and fuel quantity ratios for first- and second-stage injection.

For the optimization, a basic understanding is necessary—especially as to the effects of the additional parameters on combustion process—because these parameters greatly affect the formation of fuel-air mixture and therefore vary the heat release process and formation of soot, NOx and other combustion products in a complicated manner compared to single-injection cases. Regarding the mixture formation in two-stage injection, Bruneaux measured the distributions of OH, PAH and soot in sprays for several injection dwells [19]. However, the fundamental data are still insufficient to fully understand the relation among the injection parameters, mixture formation and combustion process. From this point of view, the present study aims to clarify the effects of two-stage injection under simplified conditions—excluding the influence of in-cylinder flow and change in cylinder volume. For this purpose, a constant-volume vessel is employed to simulate partial PCCI combustion with two-stage injection. The interval of injections and fuel-quantity ratios were vary under the conditions of ordinary (21%) and lower (15%) ambient O_2 concentrations. Heat release rate, shadowgraph images and NOx concentration are acquired. Based on these data, mechanisms are discussed on the influence of the above parameters on mixture formation, development of flames, as well as formation and decay of NOx and soot.

EXPERIMENTAL

CONSTANT-VOLUME VESSEL

The experimental system and measurement methods used in the present study are basically the same as those reported in the previous study [20]. A constant-volume vessel is used to generate a high-temperature and high-pressure environment for fuel spray ignition. The vessel has a combustion chamber with a diameter of 80 mm and a depth of 30 mm, as shown in Fig. 1. A lean premixed gas prepared in another vessel is introduced into the combustion chamber through an intake valve. Then, the mixture is ignited by an automotive spark plug to form the environment necessary for the spontaneous ignition of a fuel spray. The premixed gas consists of C_2H_4, H_2, O_2 and N_2. The mole fraction of each species and the total pressure are selected so as to obtain the target ambient temperature, pressure and oxygen mole fraction at the start of fuel injection. In the present study, the ambient pressure and temperature at first-injection timing are set at 2 MPa and 900 K. By selecting such an ambient condition, PCCI-like combustion is realized, in which most of the injected fuel burns in the premixed combustion phase in the case of single injection. The ambient oxygen mole fraction at the start of injection is set at 21% for an ordinary combustion condition and at 15% to simulate EGR conditions. It should be noted that the oxygen mole fraction is reduced by replacing oxygen with nitrogen in the lean

premixed gas. The heat capacity of ambient gas is hardly influenced by changing the oxygen mole fraction, unlike the case of an actual EGR.

Normal heptane with a cetane number of around 57 is used as fuel. The cetane number of light diesel fuel used in Japan (JIS #2 grade) is between 55–60. Therefore, n-heptane has similar ignitability to diesel fuel. In the experiments, n-heptane is injected toward the center of the combustion chamber using a single-hole nozzle with an electrically controlled common-rail injection system (Denso ECD-U2P). Here, the nozzle orifice diameter (straight hole) is 0.2 mm, and the injection pressure is fixed at 120 MPa. The total amount of injected fuel is 19.5 mg, which corresponds to an overall equivalence ratio of 0.26 at an ambient oxygen mole fraction of 21%. The fuel quantity used in the first injection is varied between 1.95 to 7.8 mg (10 to 40% of total fuel). The injection dwell t_{int} is varied between 0.5 to 2.0 ms. Here, the injection dwell is defined as the interval between the end of the first injection and the start of the second injection, as shown in Fig. 2. For comparison, single-injection tests are also carried out.

The fuel injection mass rate is measured from the pressure history when the fuel is injected into a small constant-volume chamber filled with fuel. The injection rates dm_f/dt and the needle lifts h for various first-injection quantities m_1 with an injection dwell t_{int} of 1.0 ms are shown in Fig. 3. For the smallest first-injection quantity, m_1 = 1.95 mg, the maximum rate of the first injection is slightly lower than that of the second injection due to the short duration of needle lift. On the other hand, the maximum injection rates are comparable to a second injection for m_1 = 3.9 and 7.8 mg. The mean injection rate in the first-injection stage becomes lower as m_1 decreases due to the increasing contribution of the rise and fall processes.

HEAT RELEASE ANALYSIS AND SHADOWGRAPH IMAGING

A piezoelectric pressure transducer (Kistler 6052A) and a Hall-effect displacement sensor were used to detect pressure changes in the combustion chamber and the needle lift of the fuel injector. The heat release rate was calculated from the pressure based on a single-zone model. The effect of heat loss to the combustion chamber wall was compensated for using a heat-transfer rate obtained from the pressure record with no injection.

To show the mixture formation and combustion process, high-speed shadowgraph photographs were taken. Collimated parallel light from an Xenon light source was passed through fused-silica windows fitted in both sides of the combustion chamber. Images were captured by a high-speed digital video camera (Photron Fastcam SA5) at 20,000 fps. The acquired images were analyzed to obtain the histories of the luminous flame area to enable investigation of the formation and decay of soot in the combustion chamber. The exposure time, the lens aperture, camera sensitivity and the intensity of illumination were set at the same values for all the photographs.

TOTAL GAS-SAMPLING APPARATUS

The total gas-sampling apparatus used to freeze fast-chemical reactions during combustion and obtain the NOx concentration is shown in Fig. 4 [20-23]. A dilution tank is connected to the combustion chamber via a diaphragm. The dilution tank has a volume of approximately 4,000 cm^3 and is filled with nitrogen, which dilutes and cools the sample gas. In all experiments, the dilution ratio is fixed at 5.5 on a mass basis. In this apparatus, a needle actuated by an air-cylinder ruptures the diaphragm. The rupture timing can be set as desired by selecting the energizing timing of the pneumatic valve connected to the air-cylinder. When the diaphragm is ruptured, gas inside the combustion chamber rapidly expands into the dilution tank and is cooled

to below 600 K, quenching the chemical reactions. The collected gas is then analyzed using a chemiluminescent NOx analyzer (Yanaco ECL-88A) to obtain the NOx ($NO+NO_2$) concentration.

RESULTS AND DISCUSSION

EFFECTS OF FUEL-QUANTITY RATIO AND INJECTION DWELL TIME ON HEAT RELEASE RATE

ORDINARY AMBIENT OXYGEN MOLE FRACTION CASE (r_{O2} = 21%)

First, the effects of first-injection quantity and injection dwell on pressure in the combustion chamber and heat release rate were investigated at an ambient oxygen mole fraction r_{O2} of 21%.

The effective pressure p_f-p_a, thermodynamic mean temperature in the combustion chamber T, heat release rate dQ/dt, and output of needle lift sensor h in the case of first-injection quantity m_1 = 1.95 mg, and injection dwell t_{int} = 2.0 ms are shown in Fig. 5. Here, p_f-p_a was calculated from the measured pressure p_f and the pressure p_a with no injection, where p_a corresponds to the pressure decay due to heat loss to the combustion chamber walls. Thus, p_f-p_a indicates the pressure change due to heat release and absorption, excluding the effect of heat loss. p_f-p_a is zoomed around 0 MPa to examine the change in p_f-p_a around ignition timing. The origin of time t in the horizontal axis is set at the start of the second injection. Such a representation is convenient for a comparison of main (second-stage) heat release processes as shown in the next graph. p_f-p_a starts to decay just after the start of the first injection due to heat absorption of the spray, and then shows a gradual rise due to low temperature reaction, and finally a rapid increase due to high temperature reaction. Heat release rates by first and second injection are separated in this case. The fuel from the first injection is ignited prior to the start of the second injection after a long ignition delay, which indicates the fuel burns in a premixed combustion mode. The ignition delay of the second-injection fuel is very short, and an initial peak for the heat release rate is hardly observed due to the temperature rise in the first-stage heat release. Almost all the fuel from the second injection burns in a diffusion combustion mode.

The effects of injection dwell t_{int} for m_1 = 1.95 mg are shown in Fig. 6. In the case of single-stage injection, a large part of the fuel burns in a premixed combustion phase. Under the conditions of this experiment, however, a small part of the fuel is provided for the diffusion combustion phase indicated by a very low heat release rate after a large peak, because ignition takes place before the end of injection. The combustion mode can be changed by changing injection dwell in the case of two-stage injection. As mentioned above, the heat release process is separated into two parts for a long injection dwell of t_{int} = 2.0 ms: the first part with premixed combustion of fuel from the first-stage injection, and the second part with diffusion combustion of secondly injected fuel. On the other hand, in the case of the shortest injection dwell of t_{int} = 0.5 ms, the heat release processes by both injection stages seem to be merged. The decrease in p_f-p_a stops at 0.8 ms after the start of first injection, which means the chemical reactions shift to an exothermic stage. However, p_f-p_a begins to decrease again due to heat absorption caused by the spray of the second-stage injection. This indicates the ignition of the first-stage-injection spray is prevented. As a result, the fuel-air mixture created by the first injection ignites with the mixture from the second injection, and therefore the peak of the initial heat release rate is higher than that for t_{int} = 2.0 ms. The heat release process of t_{int} = 1.0 ms is intermediate between t_{int} = 0.5 and 2.0 ms. Thus, the peak level of the initial heat release rate is controlled by the injection dwell.

The results of m_1 = 3.9 and 7.8 mg are shown in Figs. 7 and 8, respectively. According to the increase in the first-injection quantity, the peak of the first heat release increases. In the case of the largest first-injection

quantity m_1 = 7.8 mg, the change in the initial heat release is small, while the peak is lower compared to single injection.

The maximum initial heat release rate dQ/dt_{max} and ignition delay against injection dwell t_{int} are shown in Fig. 9. Here, t_h means the start of a rapid increase in the heat release rate, which corresponds to hot flame initiation [20], and t_{j2} is the start of second injection. t_h-t_{j2} indicates the ignition timing based on the start of the second injection. Decreasing first-injection quantity reduces dQ/dt_{max}. The reduction in dQ/dt_{max} results in a lower maximum pressure rise rate, which would result in lower combustion noise. For m_1 = 1.95 mg, a longer t_{int} result in a lower dQ/dt_{max}. However, a t_{int} longer than 1.0 ms for m_1 = 3.9 mg cannot reduce dQ/dt_{max}. This is because a long t_{int} results in the ignition of first-injection fuel before the start of second injection (t_h-t_{j2} < 0). In such a case, the initial heat release rate is determined only by the first injection. In the case of the largest first-injection quantity of m_1 = 7.8 mg, the hot flame of the first injection starts before the start of the second injection in all cases, because the interval between first- and second-injection start is long. Therefore, the peak of the first heat release cannot be controlled by changing the injection dwell.

REDUCED AMBIENT OXYGEN MOLE FRACTION CASE (r_{O2} = 15%)

Further experiments were carried out for the reduced ambient oxygen mole fraction, r_{O2} = 15%. The heat release rates, temperatures and pressures for injection dwells of 0.5, 1.0 and 2.0 ms, and for first-injection quantities of 1.95, 3.9 and 7.8 mg are shown in Fig. 10. In all cases, the heat release rates of the first and second injection are not completely separated because of the longer ignition delay of the first injection. Regardless of m_1, the effective pressure p_f-p_a shows a two-step decrease for t_{int} = 0.5 and 1.0 ms, which was observed at t_{int} = 0.5 ms in the case of r_{O2} = 21%. For the shortest injection dwell of t_{int} = 0.5 ms, the steep rise in the heat release rate starts around the end of the second injection; therefore, most of the injected fuel burns during the premixed combustion phase. For the longest injection dwell of t_{int} = 2.0 ms, heat release starts around the start of the second injection, which results in diffusion combustion of the fuel from the second injection.

The maximum initial heat release rate dQ/dt_{max} and ignition delay based on second-injection start t_h-t_{j2} against injection dwell t_{int} are shown in Fig. 11. In most cases, dQ/dt_{max} is higher compared to r_{O2} = 21%. This is because the ignition delay of the first-injection fuel becomes long, which brings a larger amount of second-injection fuel into the premixed combustion phase. As in the case of r_{O2} = 21%, a smaller first-injection quantity results in a lower dQ/dt_{max}. Unlike the case of r_{O2} = 21%, dQ/dt_{max} decreases as t_{int} is longer even for the largest m_1, because t_h-t_{j2} is positive.

SHADOWGRAPH IMAGES

High-speed shadowgraph photographs of sprays and flames were taken to show the relation between mixture formation and the heat release process. Images taken under the same conditions as in Figs. 5-11 are shown in Figs. 12-21. The time displayed on each image represents the time from the second injection, and the time in parenthesis indicates the time from the first injection. The heat release rate history is also shown in the lower part of the figures, with corresponding image numbers.

ORDINARY AMBIENT OXYGEN MOLE FRACTION CASE (r_{O2} = 21%)

In the case of single injection (Fig. 12), the spray tip reaches the chamber wall at around t = 1 ms (image No. 1), and a nonluminous flame is observed in the mixture spreading along the wall (marked “A”, No. 2). Then, a luminous flame appears (No. 3) and spreads along the wall (Nos. 3-5). The luminous flame disappears in image No. 6, which corresponds to the end of weak heat release during the diffusion combustion phase.

In the case of two-stage injection with the smallest first-injection quantity, m_1 = 1.95 mg and the longest injection dwell, t_{int} = 2.0 ms (Fig. 13), the mixture from the first injection ignites after a long ignition delay at t = -0.8 ms (marked "A", No. 2). A nonluminous flame appears and the burned gas region spreads in the bottom and center area of the chamber (Nos. 2-3). The second spray reaches the burned gas region at around t = 0.4 ms, then a luminous flame immediately appears from the tip of the spray (No. 5). The area with high luminosity increases and then starts to decrease from image No. 7, in which the heat release rate is decaying in the diffusion combustion phase. The luminous flame almost disappears up to t = 4.0 ms (No. 8). The long time lag between the combustion of the first injection and the ignition of the fuel from the second injection results in the separated heat release.

For the shorter injection dwell, t_{int} = 1.0 ms (Fig. 14), the second injection starts at almost the same time as the ignition of the first injection (marked "A", No. 2). The second spray starts to burn just after it reaches the spreading burnt gas region generated by the first injection (marked "B", No. 3), then a luminous flame appears (No. 4). The luminous flame remains up until the end of heat release (No. 8). In the case of the shortest injection dwell, t_{int} = 0.5 ms (Fig. 15), the second spray penetrates into the mixture formed by the first injection. The mixtures from the first and second injections are mixed with each other and then ignite (marked "A", No. 3), which results in a higher peak heat release rate compared to the cases of longer t_{int}. Just after the nonluminous flame starts to expand, a luminous flame appears (No. 4).

Thus, in the case of a small first-injection quantity, the difference in ignition timings of the first and second injections affects the amount of mixture participated in the initial combustion and changes the peak level of the heat release rate.

In the case of the largest amount of first-injection quantity, m_1 = 7.8 mg with the longest injection dwell, t_{int} = 2.0 ms (Fig. 16), the development of sprays and flames is qualitatively similar to that for m_1 = 1.95 mg with the same t_{int} (Fig. 13). However, the burned gas region formed by the first injection is significantly larger due to the increased injection quantity. In addition, the decay of the luminous flame is faster. This is because the fuel quantity in the second injection is reduced. The second sprays reaches the burned gas region after the region fully develops. On the other hand, for the shorter dwells, t_{int} = 1.0 ms and t_{int} = 0.5 ms (Figs. 17 and 18), the burned gas region is still growing when the second spray reaches there. Obviously, for t_{int} = 0.5 ms, the second spray is engulfed by the rapidly expanding nonluminous flame. The encounter between the second spray and the burned gas is within the increasing process of initial heat release for t_{int} = 0.5 ms (Fig. 18, No. 4), on the other hand, within the decaying process for t_{int} = 1.0 ms (Fig. 17, No. 5). In spite of such a difference, the peak of the initial heat release is almost the same, regardless of t_{int}. This is because the second spray starts to burn in diffusion combustion mode, and therefore releases only a small amount of heat during the initial stage of combustion.

Thus, in the case of a large first-injection quantity, the peak level of the heat release rate is not controlled by the injection dwell. As for the case of a medium quality of fuel being used in the first injection, m_1 = 3.9 mg, the characteristics of mixture formation and flame development are intermediate between the case of m_1 = 1.95 mg and m_1 = 7.8 mg.

REDUCED AMBIENT OXYGEN MOLE FRACTION CASE (r_{O2} = 15%)

In the case of a single injection with a low oxygen mole fraction of r_{O2} = 15% (Fig. 19), ignition occurs after a significantly longer ignition delay than for r_{O2} = 21% (marked as "A", No. 4). Therefore, the heat release pattern consists only of the premixed combustion phase, and a luminous flame is not observed.

For two-stage injection with the shortest injection dwell, t_{int} = 0.5 ms and m_1 = 1.95 mg (Fig. 20), the mixture from the first injection becomes very lean before the second spray reaches there (No. 2). The second spray penetrates into the lean mixture (No. 3), then ignition occurs in the region aside from the spray just before the end of second injection (marked "A", No. 5), and the nonluminous flame rapidly spreads (Nos. 5-6). Up to ignition, the mixture from the first injection is thoroughly leaned out and the second spray entrains a certain amount of surrounding gas. Therefore, the premixed combustion phase is predominant in the heat release process, and only a small amount of luminous flame is observed. Although the heat release pattern is similar to that in the single-stage injection case, the peak of the heat release rate is lower. This is because part of the fuel from the second injection undergoes diffusion combustion as indicated by the appearance of the weak luminous flame and the low heat release rate in the later combustion stage. On the other hand, the peak heat release rate is much higher compared to the results for the same t_{int} and m_1 under the condition of ordinary oxygen mole fraction (Fig. 15). This is due to the increase in the leaner mixture as already mentioned.

For the longest injection dwell, t_{int} = 2.0 ms (Fig. 21), unlike the case of the shorter dwell t_{int} = 0.5 ms (Fig. 20), the mixture from the first injection ignites (marked "A", No. 4) just after the start of second injection. The second injection spray penetrates into the burned gas (No. 5), then immediately ignites. Therefore, the combustion process is dominated by diffusion combustion accompanying luminous flame (Nos. 6-11). Compared to the case of t_{int} = 0.5 ms, the flame has significantly higher luminosity.

The observations obtained here were basically similar in the cases of a larger first-injection quantity, m_1 = 3.9 and 7.8 mg.

LUMINOUS FLAME AREA

The results up to this point indicate that the combustion of fuel from the first injection is not a direct cause of soot formation, judging from the fact that a nonluminous flame is always observed. The combustion of fuel from the second injection seems to be responsible for soot formation. To confirm this and to investigate the effect of injection dwell and quantity on soot formation, the areas of luminous flame were derived by the binarization of shadowgraph images, and the influence of the injection and ambient conditions are discussed. The threshold level at which to binarize the images was set to a relatively high value—intermediate between the background level inside the combustion chamber and the maximum gray level. Therefore, observations of a weak luminous flame as in image No. 8 on Fig. 20 are not counted in this area.

The areas of luminous flame S_{LF} and the heat release rates for the first-injection quantities, m_1 = 1.95 and 7.8 mg, under the condition of an ambient oxygen mole fraction r_{O2} of 21% are shown in Fig. 22. The single-injection case shows a low S_{LF} with a short duration. On the other hand, two-stage injection cases provide a high S_{LF} with longer durations. This tendency is more remarkable for a smaller first-injection quantity because a larger amount of fuel is injected during the second stage, which burns in the diffusion combustion phase.

For m_1 = 1.95 mg, the start of rise in S_{LF} is the earliest for t_{int} = 1.0 ms. This is because the second spray is ignited by the spreading flame from the first injection, as already mentioned. On the other hand, for t_{int} = 0.5 ms, the second spray ignites after merging with the mixture formed by the first injection; therefore, the appearance of a luminous flame is delayed. In spite of such a difference, the end timings of S_{LF} are not significantly different. The maximum of S_{LF} is lower for t_{int} = 2.0 ms compared to shorter t_{int}. This is probably because the longer injection dwell makes the mixture from the first spray leaner, and therefore the amount of rich mixture is reduced when the second spray entrains the burned gas. Further investigation is required to confirm this assumption.

For m_1 = 7.8 mg, formation of soot in the diffusion combustion of the second injection is reduced owing to the reduced amount of second-injection fuel. With this effect, the peak levels or the durations of S_{LF} are reduced compared to the case of m_1 = 1.95 mg. On the other hand, the mixture from the first injection is not sufficiently leaned out due to the increased quantity of first-injection fuel. As stated in the explanation for Figs. 16-18, this causes the second sprays to undergo fully diffusional combustion regardless of t_{int}. As a result, the duration of S_{LF} is almost the same for all t_{int} as shown in Fig. 22. The trend of S_{LF} is similar in the case of m_1 = 3.9 mg.

The results for the reduced oxygen mole fraction case, r_{O2} = 15% are shown in Fig. 23. A luminous flame was not observed for a single injection. Of the two-stage injection data, the shortest injection dwell (t_{int} = 0.5 ms) also provides zero S_{LF} in the case of a small first-injection quantity, m_1 = 1.95 mg, although weak luminous flames are observed in the diffusion combustion phase as shown in Fig. 20. This is because most of the fuel burns in the premixed combustion phase in these cases. As the injection dwell increases, S_{LF} increases and lasts longer, because a larger part of fuel is participated in diffusion combustion phase as already described in Fig. 21. In the case of a larger injection quantity, m_1 = 7.8 mg, the durations of S_{LF} are obviously longer for t_{int} = 2.0 ms. The earlier decay of turbulence due to the short second-injection duration is a reason for this.

NOx MASS HISTORY AND FINAL NOx MASS

To identify the effects of injection dwell and fuel-quantity ratio on the history of NOx mass, total gas-sampling experiments were carried out under the same conditions as the above experiments.

The histories of NOx mass, heat release rates dQ/dt, thermodynamic mean temperature in the combustion chamber T, and outputs of needle lift sensor on the ambient oxygen mole fraction r_{O2} of 21% are shown in Fig. 24. NOx mass from the combustion of the first injection (combustion without a second injection, marked “pilot only” in the figure) are also plotted. “pilot only” NOx was beyond the measurement limit for m_1 = 1.95 mg. For all conditions, the NOx mass starts to rise during the diffusion combustion phase. The rise rate decreases just after the end of heat release, and reaches a final level until t = 15 ms. The initial rise rates are comparable for m_1 = 1.95 and 3.9 mg. On the other hand, the rates are slightly lower for m_1 = 7.8 mg. This may be related to the slow rise in temperature after the initial premixed combustion phase. The "pilot only" NOx for m_1 = 3.9 mg is negligible, while it accounts for a significant fraction of the total NOx mass in the case of m_1 = 7.8 mg, because combustion of the first injection elevates the temperature to a high level.

The results for the reduced oxygen condition, r_{O2} = 15% are shown in Fig. 25. Unlike the case of r_{O2} = 21%, a longer t_{int} shows a lower NOx rise rate regardless of m_1. A longer t_{int} brings a larger part of second-injection fuel into the diffusion combustion phase as described in Fig. 21. This leads to the longer heat release duration; therefore, the burning gas suffers cooling from the chamber wall.

From these data, the final NOx mass $m_{NOx\,f}$ was derived, which was defined as the saturated NOx mass at a time later than 15 ms. To compensate for the difference in the amount of heat released for each condition, the final mass was divided by the released heat Q_t. The final NOx mass per released heat $m_{NOx\,f}/Q_t$ is shown in Fig. 26. On the whole, the two-stage injection cases provide a lower $m_{NOx\,f}/Q_t$ compared to single-injection cases. The shorter t_{int} gives a higher $m_{NOx\,f}/Q_t$ because a larger part of the fuel is included in the premixed combustion phase and therefore, the temperatures of the mixture become higher during the initial stage of combustion. Another possible reason is that a longer t_{int} with extended diffusion combustion phase tends to suffer a cooling effect from the chamber wall as illustrated in Fig. 25. It is expected that this effect would be more distinct in actual engines if the diffusion combustion phase were allocated during the expansion stroke, because the cooling effects for the burned gas is more intense due to the increase in cylinder volume.

Regarding the effects of m_1, the case of m_1 = 3.9 mg results in lower $m_{NOx\,f}/Q_t$ compared to other m_1 conditions. As shown in Fig. 24, the first-injection combustion of m_1 = 3.9 mg produces only a small amount of NOx. In addition, the second-injection quantity on m_1 = 3.9 mg is smaller compared to m_1 = 1.95 mg. Therefore, NOx mass on m_1 = 3.9 mg is reduced than that of m_1 = 1.95 mg. In the case of m_1 = 7.8 mg, $m_{NOx\,f}/Q_t$ would be increased due to the increased NOx mass from the first injection.

CONCLUSIONS

To clarify the effects of injection dwell and fuel-quantity ratio on the heat release process and formation of soot and NOx, an experimental study was conducted under simulated partial PCCI conditions with two-stage injection utilizing a constant-volume vessel. Heat release rates, high-speed shadowgraph photographs and NOx mass data were analyzed. From the results obtained, the following conclusions were drawn.

1. In the case of a small first-injection quantity, longer injection dwells reduce the peak of the initial heat release rate. For a very short dwell, heat absorption by the second spray suppresses ignition of the mixture from the first injection and increases the amount of combustible mixture up to ignition, leading to a higher initial heat release rate.

2. In the case of a large first-injection quantity, the peak of the initial heat release rate is not controlled by the injection dwell because the second spray is ignited by the high temperature resulting from the preceding combustion of the first-injection fuel, and therefore always burns totally in diffusion combustion mode. However, under lower ambient oxygen mole fraction conditions, the dwell influences the heat release peak, even for a larger first-injection amount as the ignition of first injection is delayed.

3. Luminous flames are not observed during combustion of first-injection fuel; however, the combustion of the second spray provides a luminous flame of longer duration than in a single-injection case. An increase in the first-injection quantity shortens the duration of the luminous flame. The influence of injection dwell is not significant for an ordinary ambient oxygen mole fraction; however, under a reduced oxygen condition, the duration and area of luminous flames increase as the injection dwell is longer.

4. In the case of an ordinary ambient oxygen mole fraction, the rates of rise in NOx mass are comparable in single-stage and two-stage injections, and are hardly influenced by the injection dwell. On the other hand, in the case of reduced oxygen conditions, the rise rate is reduced by a longer injection dwell with increasing contribution during the diffusion combustion phase.

5. Regardless of the ambient oxygen mole fraction, final NOx mass per released heat is reduced by two-stage injection, especially in the case of a long injection dwell.

In this study, attention was paid to the interaction of mixture formation and ignition in first and second injections, and to the mechanisms by which the injection dwell and fuel quantity ratio change the combustion process. Therefore, the data and discussions provided here will be informative for finding the basic strategies for combustion control through the manipulation of injection parameters in actual engines.

The above results were obtained under the simulated and simplified conditions in the constant-volume vessel. When the formation and decay of NOx and soot are considered in actual engines, additional discussion is necessary on the influence of gas motion induced by swirl, squish and others, and also on the effects of temperature change due to the change in cylinder volume.

For example, when a wide injection dwell is employed in an engine with high swirl ratio, the effect of enhancing ignition of the second-injection spray may be weakened because the flame from the first-injection spray would move from the path of the second spray. In addition, the injection dwell should be reconsidered in terms of thermal efficiency. A wide ignition dwell as 2 ms in this study will provide further NOx reduction when the second heat release is allocated in expansion stroke. However, this will cause deterioration of thermal efficiency due to a decrease in degree of constant volume.

REFERENCES

1. Akihama, K., Takatori, Y., Inagaki, K., Sasaki, S., Dean, A. M., (2002). Mechanism of Smokeless Rich Diesel Combustion by Reducing Temperature. Diesel Particulate Emissions Landmark Research 1994-2001, presented at SAE 2001 World Congress, 2001-01-0655, 2001.
2. Kanda, T., Hakozaki, T., Uchimoto, T., Hatano, J., Kitayama, N., Sono, H., (2006). PCCI Operation with Early Injection of Conventional Diesel Fuel, SAE 2005 Transactions Journal of Engines, presented at SAE 2005 World Congress & Exhibition, 2005-01-0378, 2005.
3. Enomoto, Y., Ogawa, H., Muranaka, S., Aoki, O., Kimura, S., (2003). New Combustion Concept for Ultra-Clean and High-Efficiency. Homogeneous Charge Compression Ignition (HCCI) Engines, presented at International Fuels & Lubricants Meeting & Exposition, 1999-01-3681, 1999.
4. Arjan Helmantel, Jonas Gustavsson, Ingemar G. Denbratt, I., (2006). Operation of a DI Diesel Engine with Variable Effective Compression Ratio in HCCI and Conventional Diesel Mode. SAE 2005 Transactions Journal of Engines, presented at SAE 2005 World Congress & Exhibition, 2005-01-0177, 2005.
5. Kitabatake, R., Shimazaki, N., Nishimura, T., Expansion of Premixed Compression Ignition Combustion Region by Supercharging Operation and Lower Compression Ratio Piston (in Japanese), Proceedings of 2005 JSAE Annual Congress (Fall), No.91-05, 2005, pp.17-22.
6. Kanda, T., Hakozaki, T., Uchimoto, T., Hatano, J., Kitayama, N., Sono, H., PCCI Operation with Fuel Injection Timing Set Close to TDC, presented at SAE 2006 World Congress & Exhibition, 2006-01-0920, 2006.
7. Richard M. Opat, Youngchul Ra, Manuel A. Gonzalez D., Roger Krieger, Rolf Reitz, David Foster, Russell P. Durrett, Robert M. Siewert, Investigation of Mixing and Temperature Effects on HC/CO Emissions for Highly Dilute Low Temperature Combustion in a Light Duty Diesel Engine, presented at SAE World Congress & Exhibition, 2007-01-0193, 2007.
8. Horibe, N., Takahashi, K., Kee, S.S., Ishiyama, T., Shioji, M., (2008). The Effects of Injection Conditions and Combustion Chamber Geometry on Performance and Emissions of DI-PCCI Operation in a Diesel Engine. SAE 2007 Transactions Journal of Fuels and Lubricants, presented at 2007 JSAE/SAE International Fuels and Lubricants Meeting, JSAE 20077069/SAE 2007-01-1874, 2007.
9. Arjan Helmantel, Reduction of NOx Emissions from a Light Duty DI Diesel Engine in Medium Load Conditions with High EGR Rates, presented at SAE World Congress & Exhibition, 2008-01-0643, 2008.
10. Eastwood, P., Morris, T., Tufail, K., Winstanley, T., (2008). The Effect of Multiple Fuel-Injections on Emissions of NOx and Smoke with Partially-Premixed Diesel Combustion in a Common-Rail Diesel Engine. Proceedings of Internal Combustion Engines: Performance, Fuel Economy and Emissions, 2008, pp.285-301.
11. Hashizume, T., Akagawa, H., Tsujimura, K., (1999). Emission Reduction Using Multiple Stage Diesel Combustion, Transaction of JSME, Vol.65 No.631, pp.1166-1172. (in Japanese)
12. Hashizume, T., Miyamoto, T., Akagawa, H., Tsujimura, K., (2000). Attempt of Multiple Stage Injection with EGR for High Load Operation of a Premixed Compression Ignition Engine, Transaction of JSME, Vol.66 No.641, pp.286-293. (in Japanese)

13. Hardy, W.L., Reitz, R.D., An Experimental Investigation of Partially Premixed Combustion Strategies Using Multiple Injections in a Heavy-Duty Diesel Engine. presented at SAE 2006 World Congress & Exhibition, 2006-01-0917, 2006.
14. Yong Sun, Rolf D. Reitz, Modeling Diesel Engine NOx and Soot Reduction with Optimized Two-Stage Combustion. presented at SAE 2006 World Congress & Exhibition, 2006-01-0027, 2006.
15. Christian Weiskirch, Eckart Mueller, Advances in Diesel Engine Combustion: Split Combustion. presented at SAE World Congress & Exhibition, 2007-01-0178, 2007.
16. Chad P. Koci, Youngchul Ra, Michael Andrie, Roger Krieger, David Foster, Robert M. Siewert, Russ Durrett, Multiple Event Fuel Injection Investigations in a Highly-Dilute Diesel Low Temperature Combustion Regime. presented at SAE World Congress & Exhibition, 2009-01-0925, 2009.
17. Horibe, N., Ishiyama, T., Relations among NOx, Pressure Rise Rate, HC and CO in LTC Operation of a Diesel Engine. presented at SAE World Congress & Exhibition, 2009-01-1443, 2009.
18. Sage Kokjohn, Thaddeus Swor, Michael Andrie, Rolf Reitz, (2009). Experiments and Modeling of Adaptive Injection Strategies (AIS) in Low Emissions Diesel Engines. presented at SAE World Congress & Exhibition, 2009-01-0127, 2009.
19. Bruneaux, G. and Maligne, D., Study of the Mixing and Combustion Processes of Consecutive Short Double Diesel Injections, presented at SAE World Congress & Exhibition, 2009-01-1352, 2009.
20. Yasutaka Kitamura, Sung-Sub Kee, Ali Mohammadi, Takuji Ishiyama, Masahiro Shioji, Study on NOx Control in Direct-Injection PCCI Combustion - Fundamental Investigation Using a Constant-Volume Vessel. presented at SAE 2006 World Congress & Exhibition, 2006-01-0919, 2006.
21. Mohammadi, A., Miwa, K., Kidoguchi, Y., (2001). Effects of Injection Pressure and Fuel Properties on NOx Formation during Diesel Combustion, Trans. of JSAE, vol.32, No. 4, pp.23-28. (in Japanese)
22. Miwa, K., Mohammadi, A., Kidoguchi, Y., (2001). A Study on Thermal Decomposition of Fuels and NOx Formation in Diesel Combustion Using a Total Gas Sampling Technique, Int. J. of Engine Research, Vol.2, No.3, pp.189-198.
23. Yasutaka Kitamura, Ali Mohammadi, Takuji Ishiyama, Masahiro Shioji, Fundamental Investigation of NOx Formation in Diesel Combustion under Supercharged and EGR Conditions. presented at SAE 2005 World Congress & Exhibition, 2005-01-0364, 2005.

CONTACT INFORMATION

Naoto HORIBE

Tel: +81-75-753-5269

Fax: +81-75-753-5269

Email: horibe@elan.energy.kyoto-u.ac.jp

Takuji ISHIYAMA, Professor

Tel: +81-75-753-4729

Fax: +81-75-753-4729

Email: ishiyama@energy.kyoto-u.ac.jp

ACKNOWLEDGMENTS

The authors would like to thank Toyota Motor Corporation for providing the fuel injection system.

DEFINITIONS

dm_f/dt	Injection rate
dQ/dt	Heat release rate
dQ/dt_{max}	Maximum initial heat release
h	Output of needle lift sensor
m_1	First-injection quantity
$m_{NOx\ f}$	Saturated NOx mass
$m_{NOx\ f}/Q_t$	Final NOx mass per released heat
p_a	Pressure without injection
p_f	Measured pressure
p_f-p_a	Effective pressure
Q_t	Released heat
r_{O2}	Ambient oxygen mole fraction
S_{LF}	Area of luminous flame
T	Temperature
t	Time from start of second injection
t_{int}	Injection dwell
τ_h	Start of rapid increase of heat release rate
τ_h-τ_{j2}	Ignition timing based on second-injection start
τ_{j2}	Start of second injection

FIGURES

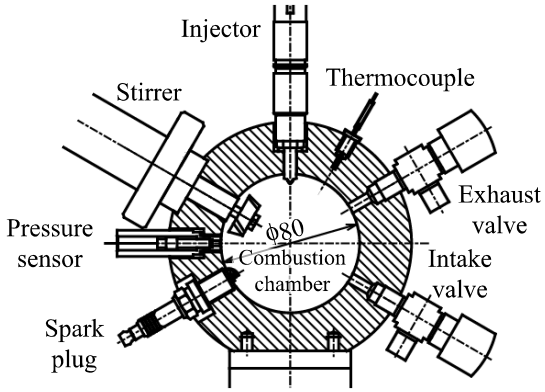

Fig. 1 Cross section of constant-volume vessel

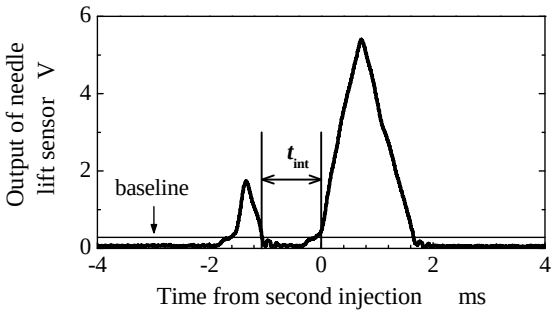

Fig. 2 Definition of injection dwell t_{int}

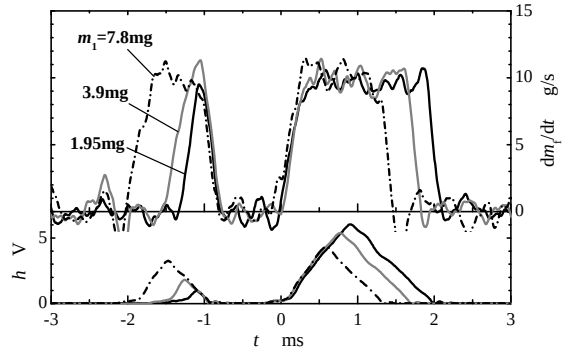

Fig. 3 Injection rates for first-injection quantity m_1 of 1.95, 3.9 and 7.8 mg with t_{int} = 1.0 ms

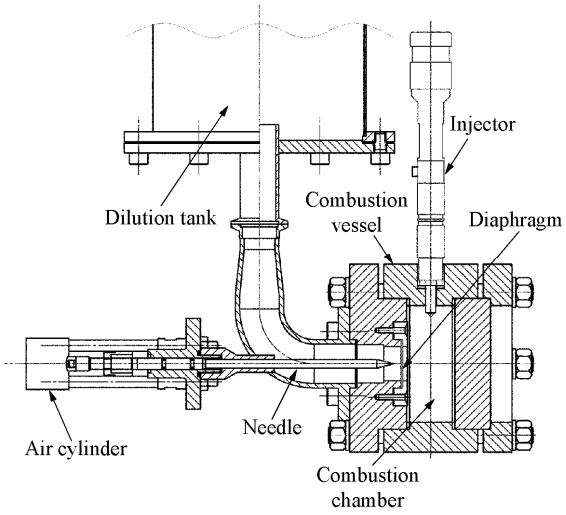

Fig. 4 Total gas-sampling apparatus

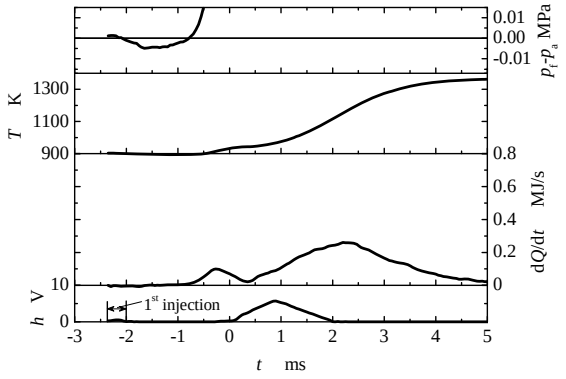

Fig. 5 Pressure, temperature, and heat release rate for first-injection quantity m_1 = 1.95 mg, injection dwell t_{int} = 2.0 ms and r_{O2} = 21%

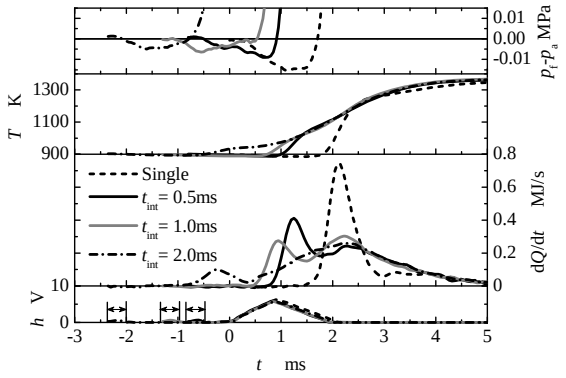

Fig. 6 Effects of injection dwell on pressure, temperature, and heat release rate (m_1 = 1.95 mg, r_{O2} = 21%)

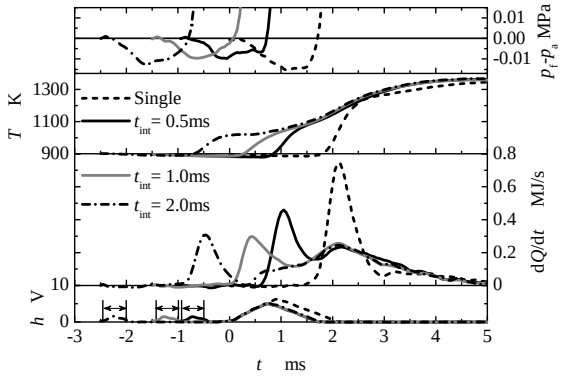

Fig. 7 Effects of injection dwell on pressure, temperature, and heat release rate (m_1 = 3.9 mg, r_{O2} = 21%)

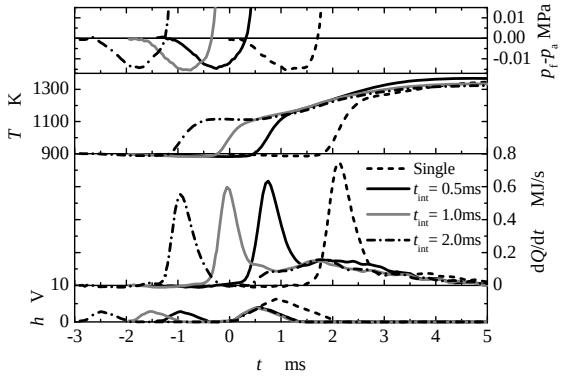

Fig. 8 Effects of injection dwell on pressure, temperature, and heat release rate (m_1 = 7.8 mg, r_{O2} = 21%)

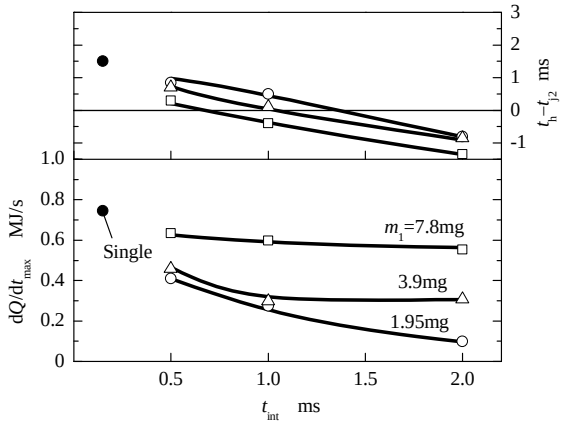

Fig. 9 Maximum initial heat release rate and hot flame delay from second-injection start (r_{O2} = 21%)

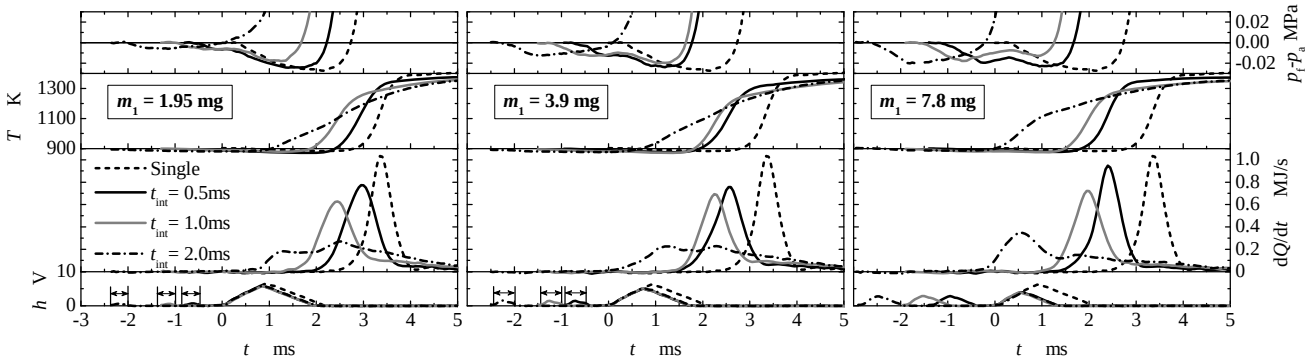

Fig. 10 Effects of injection dwell and first-injection quantity on pressure, temperature, and heat release rate (r_{O2} = 15%)

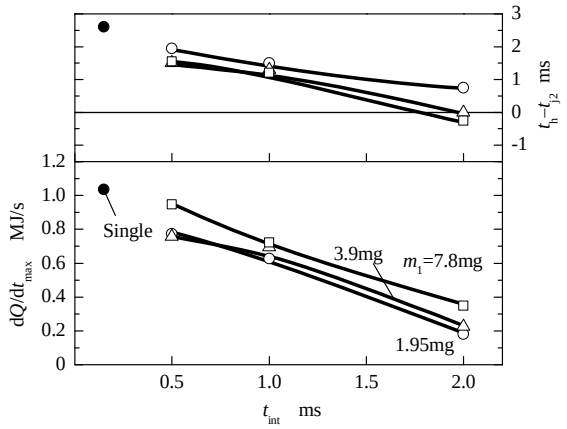

Fig. 11 Maximum initial heat release rate and hot flame delay from second-injection start (r_{O2} = 15%)

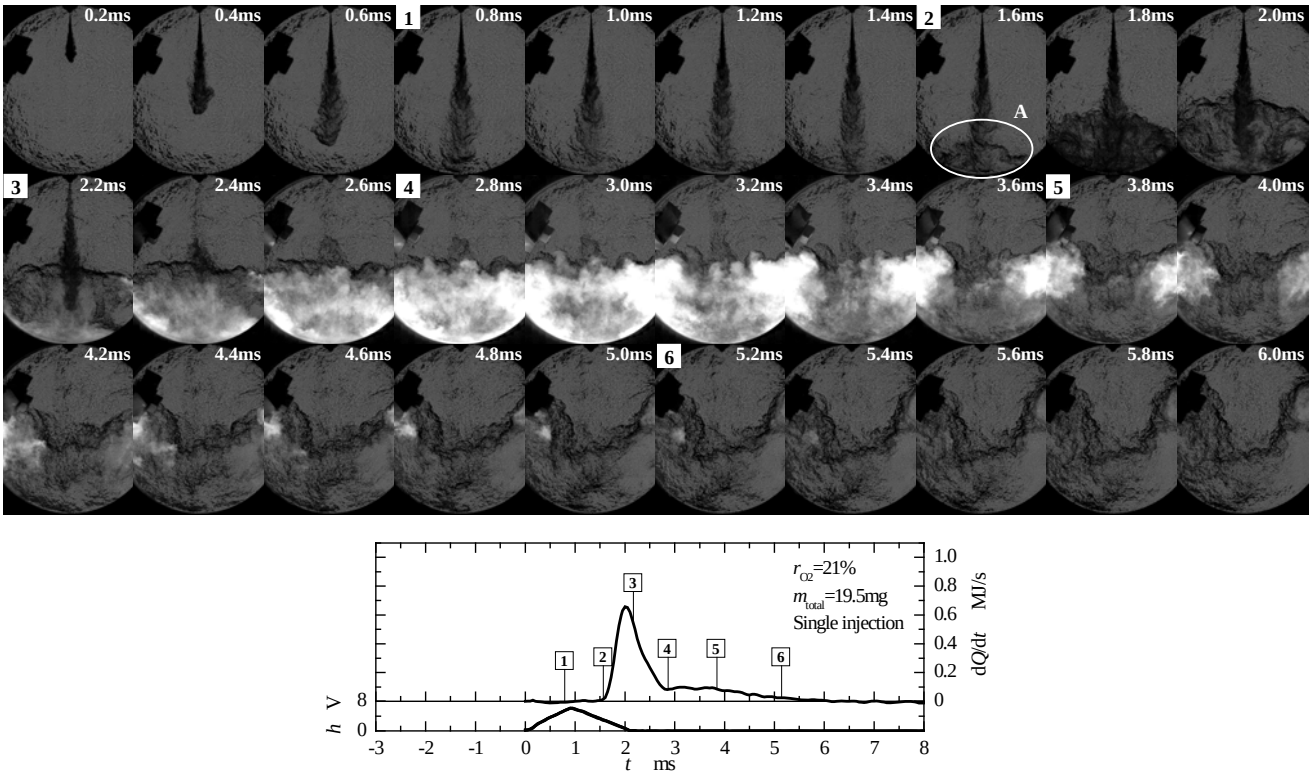

Fig. 12 Shadowgraph images and heat release rate (single injection, r_{O2} = 21%)

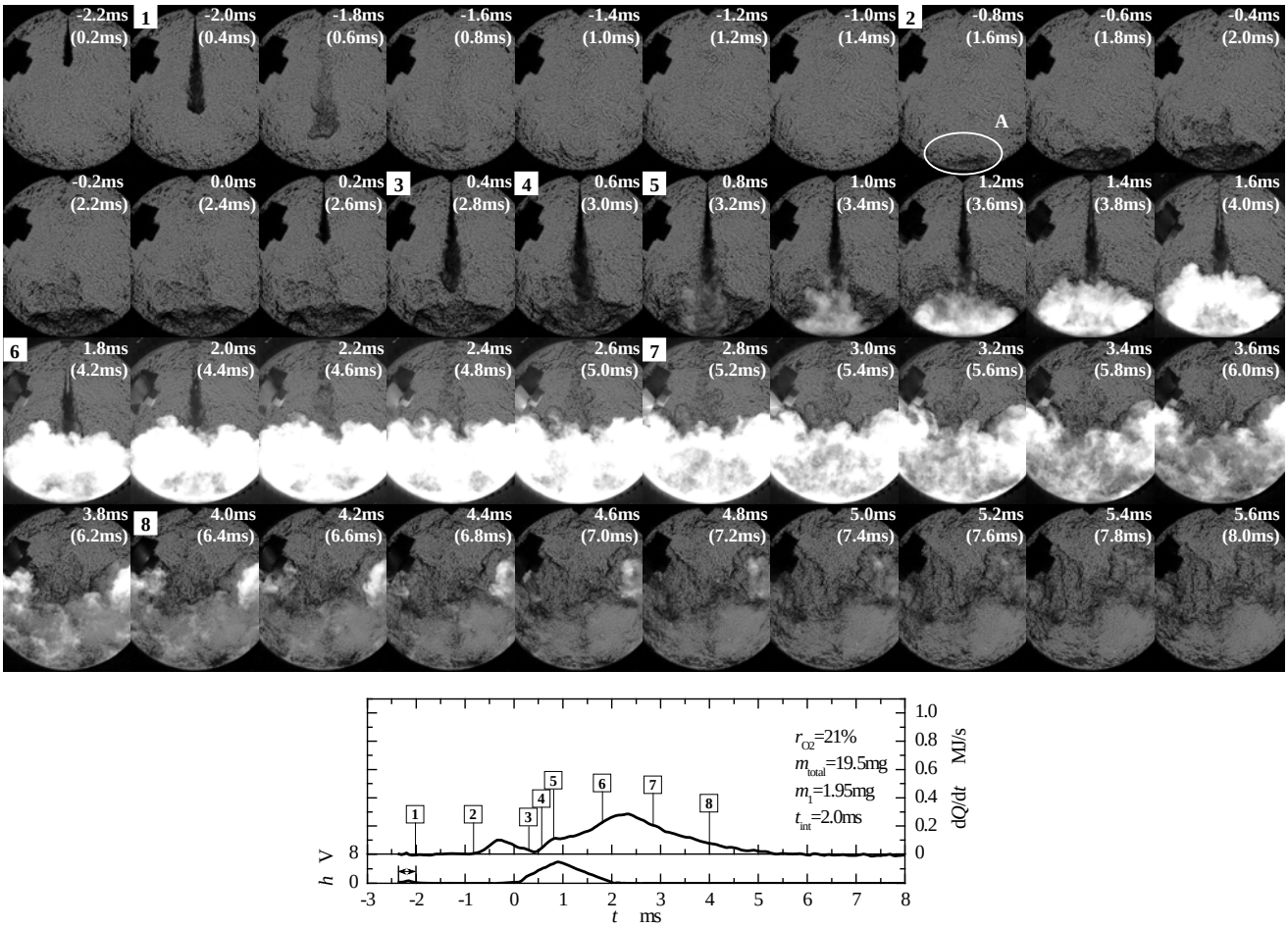

Fig. 13 Shadowgraph images and heat release rate (m_1 = 1.95 mg, t_{int} = 2.0 ms, r_{O2} = 21%)

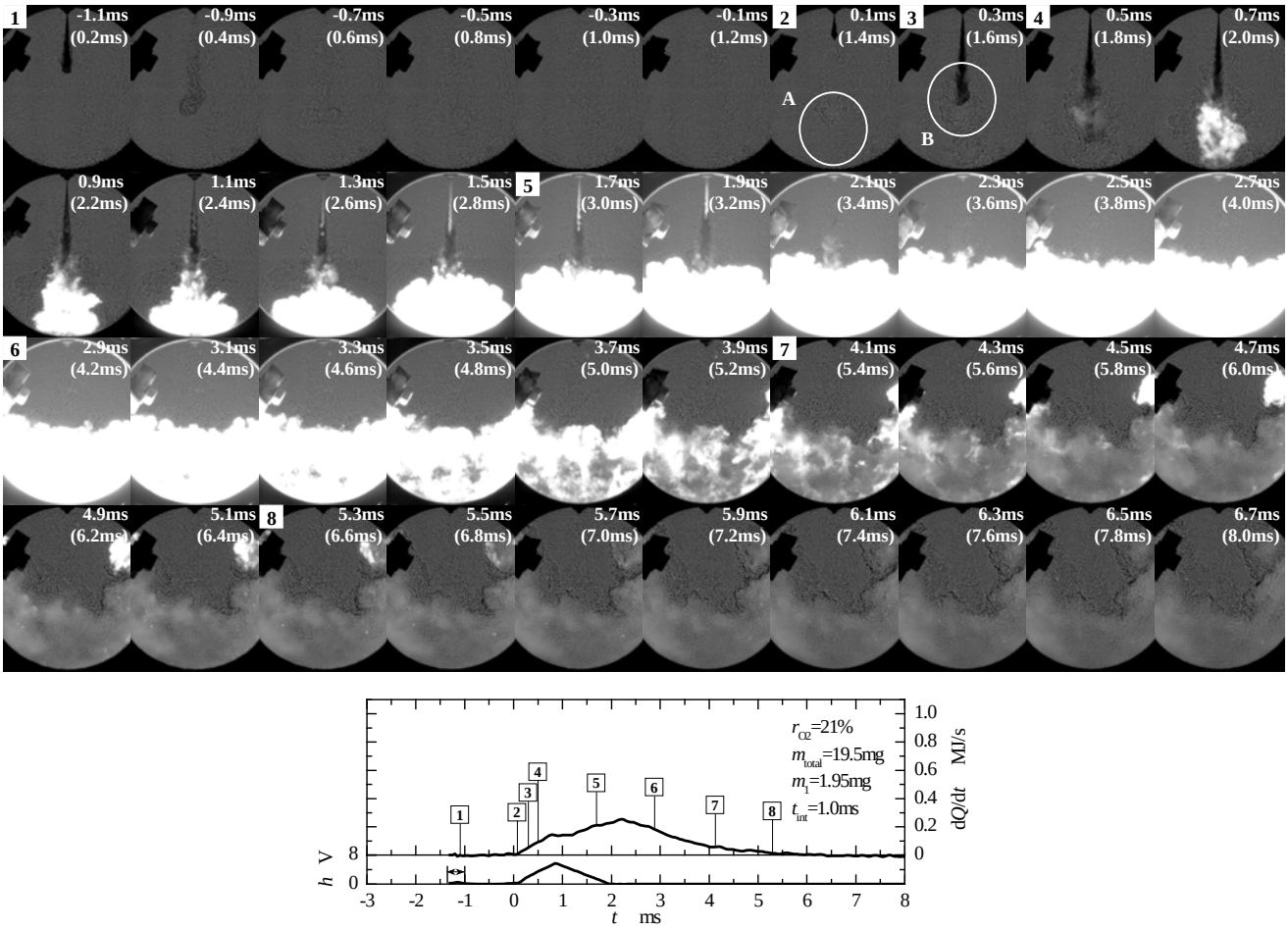

Fig. 14 Shadowgraph images and heat release rate (m_1 = 1.95 mg, t_{int} = 1.0 ms, r_{O2} = 21%)

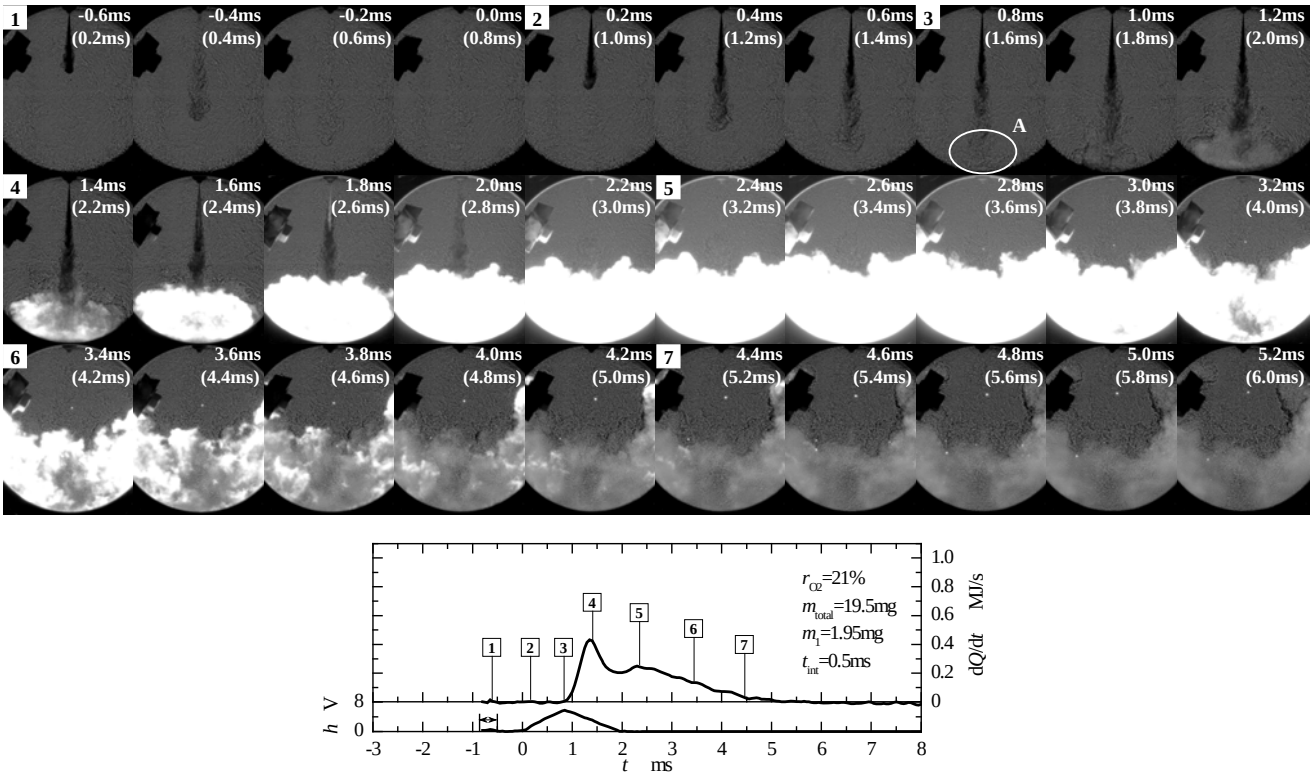

Fig. 15 Shadowgraph images and heat release rate (m_1 = 1.95 mg, t_{int} = 0.5 ms, r_{O2} = 21%)

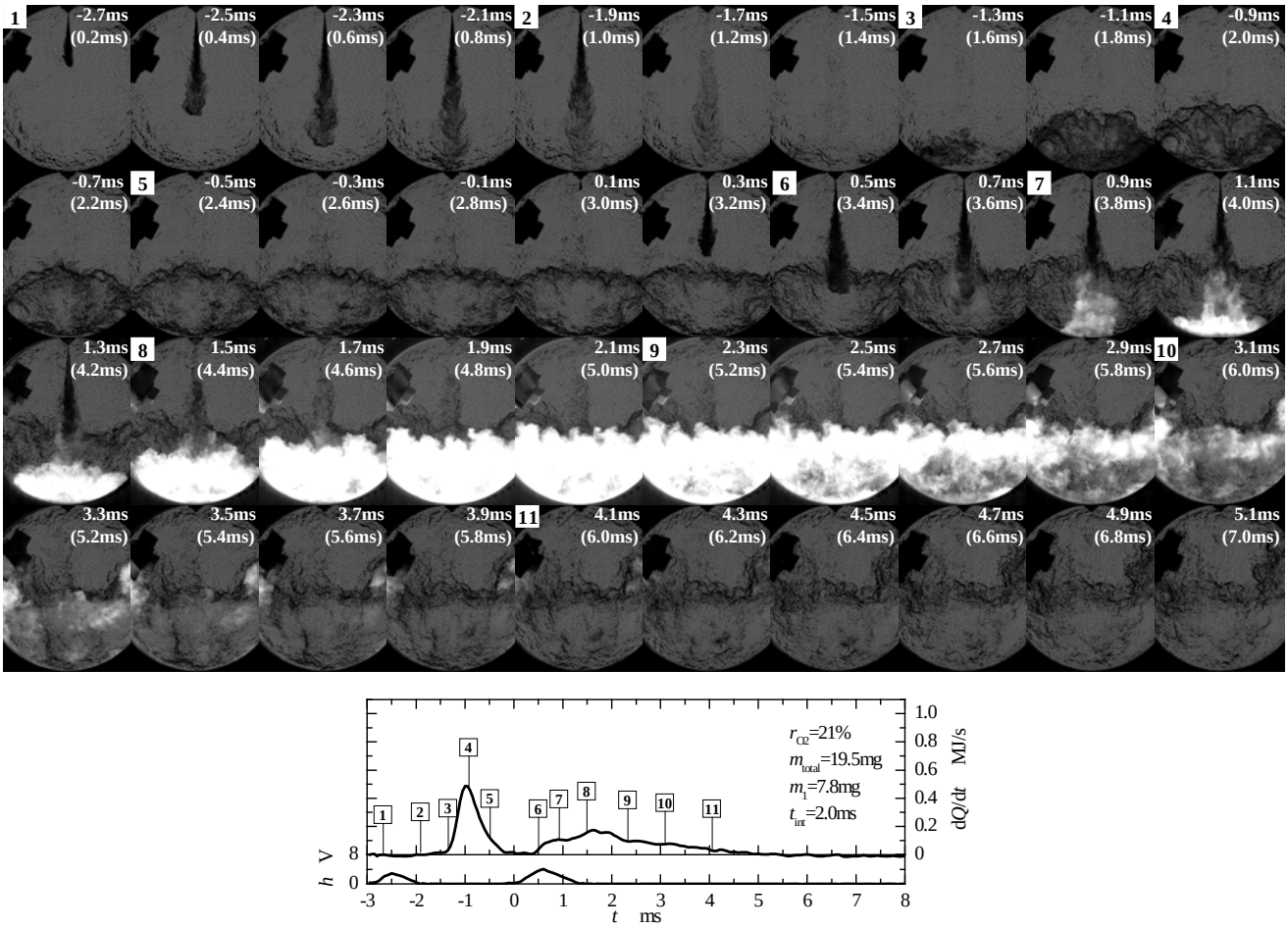

Fig. 16 Shadowgraph images and heat release rate (m_1 = 7.8 mg, t_{int} = 2.0 ms, r_{O2} = 21%)

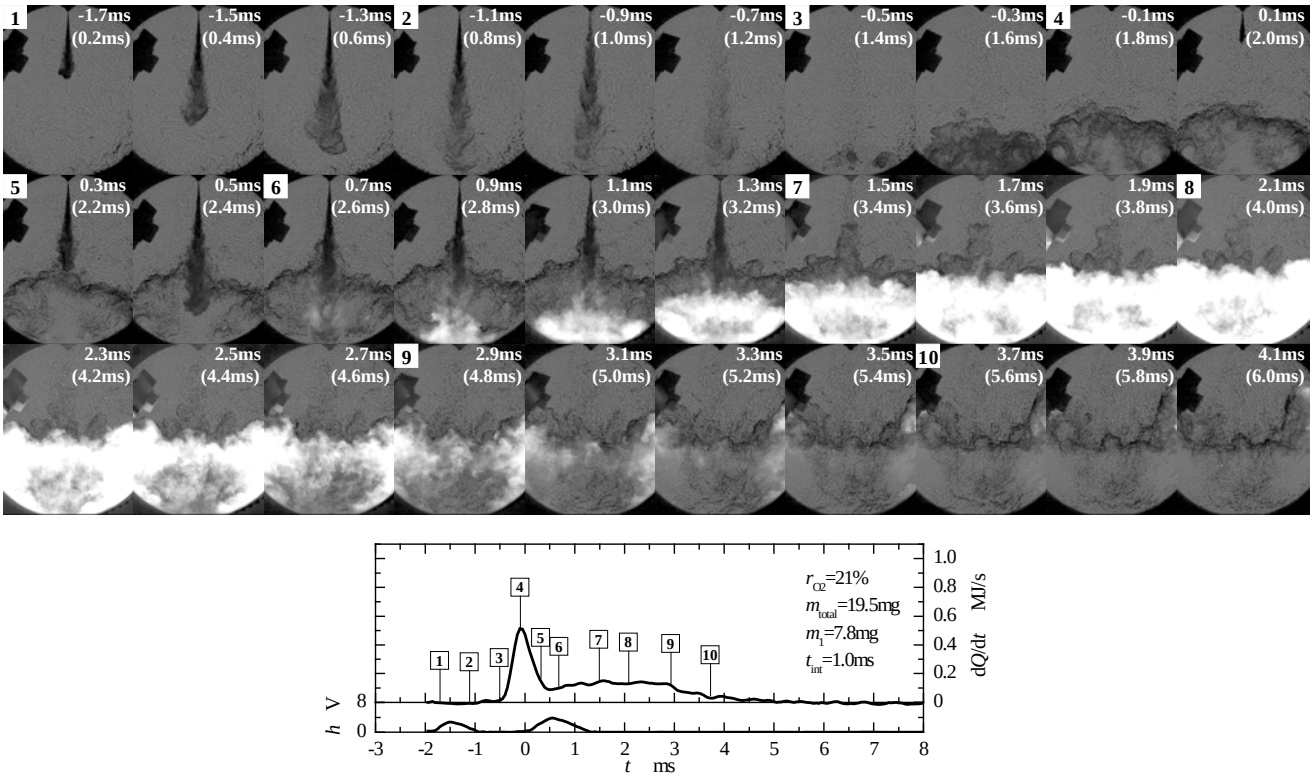

Fig. 17 Shadowgraph images and heat release rate (m_1 = 7.8 mg, t_{int} = 1.0 ms, r_{O2} = 21%)

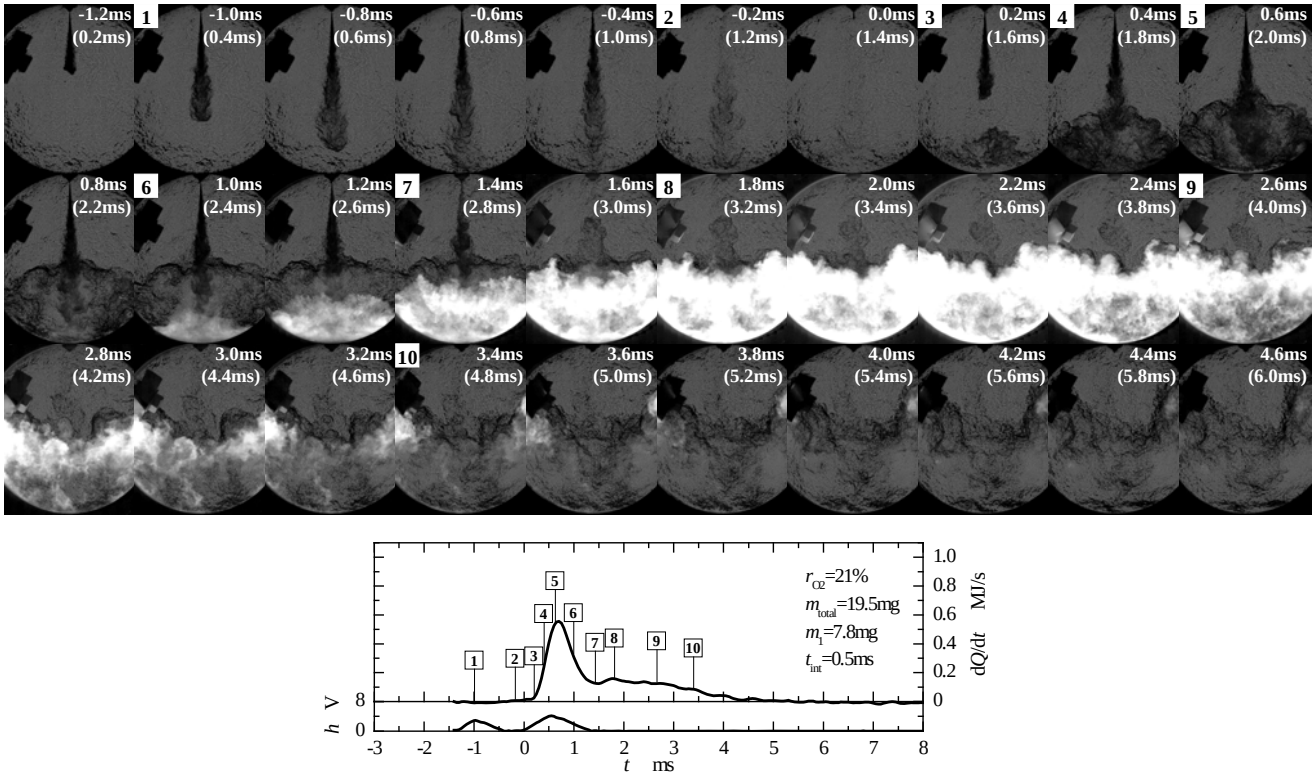

Fig. 18 Shadowgraph images and heat release rate (m_1 = 7.8 mg, t_{int} = 0.5 ms, r_{O2} = 21%)

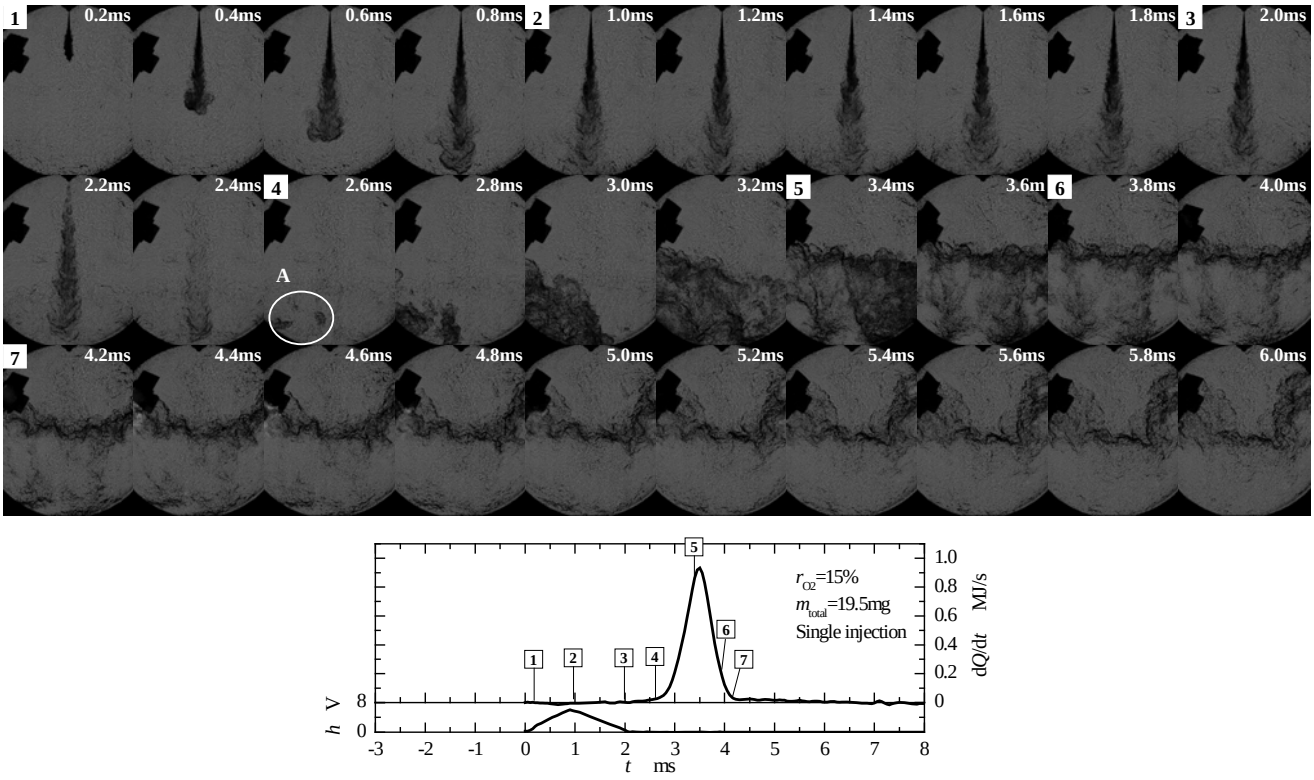

Fig. 19 Shadowgraph images and heat release rate (single injection, r_{O2} = 15%)

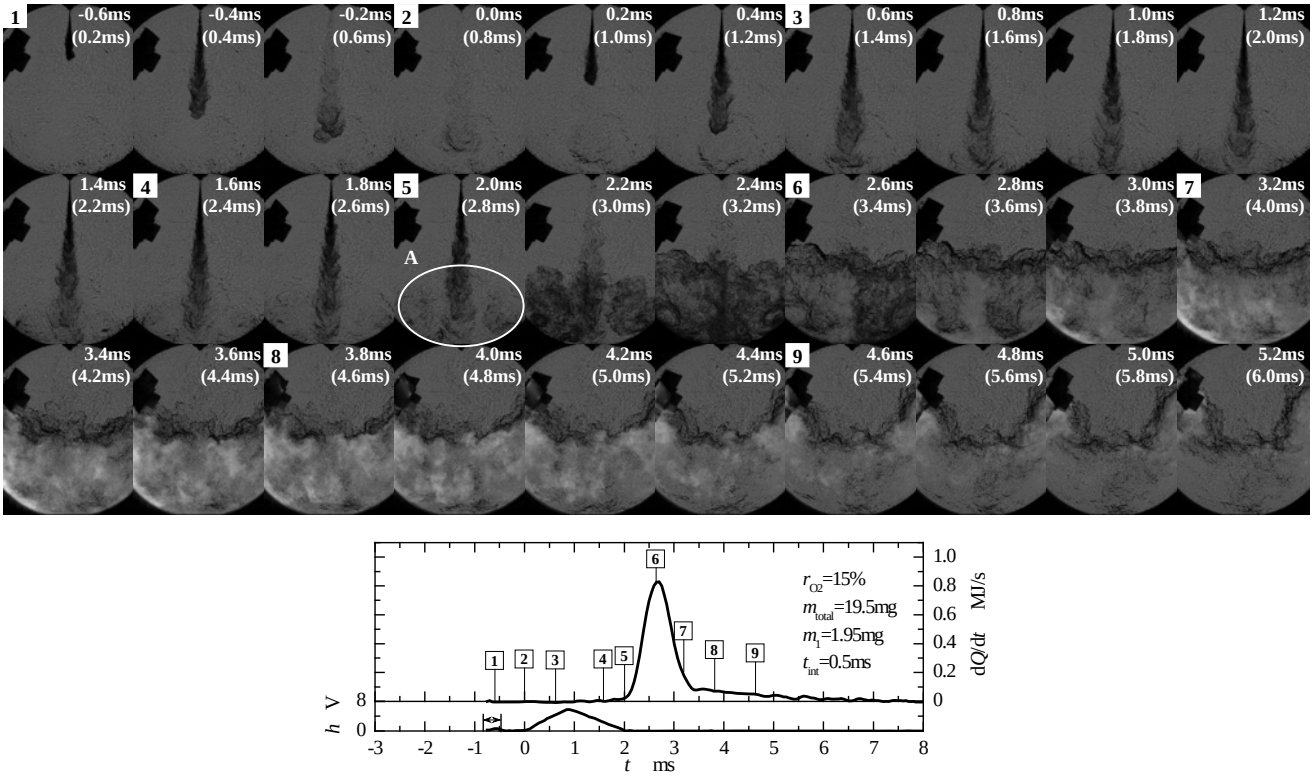

Fig. 20 Shadowgraph images and heat release rate (m_1 = 1.95 mg, t_{int} = 0.5 ms, r_{O2} = 15%)

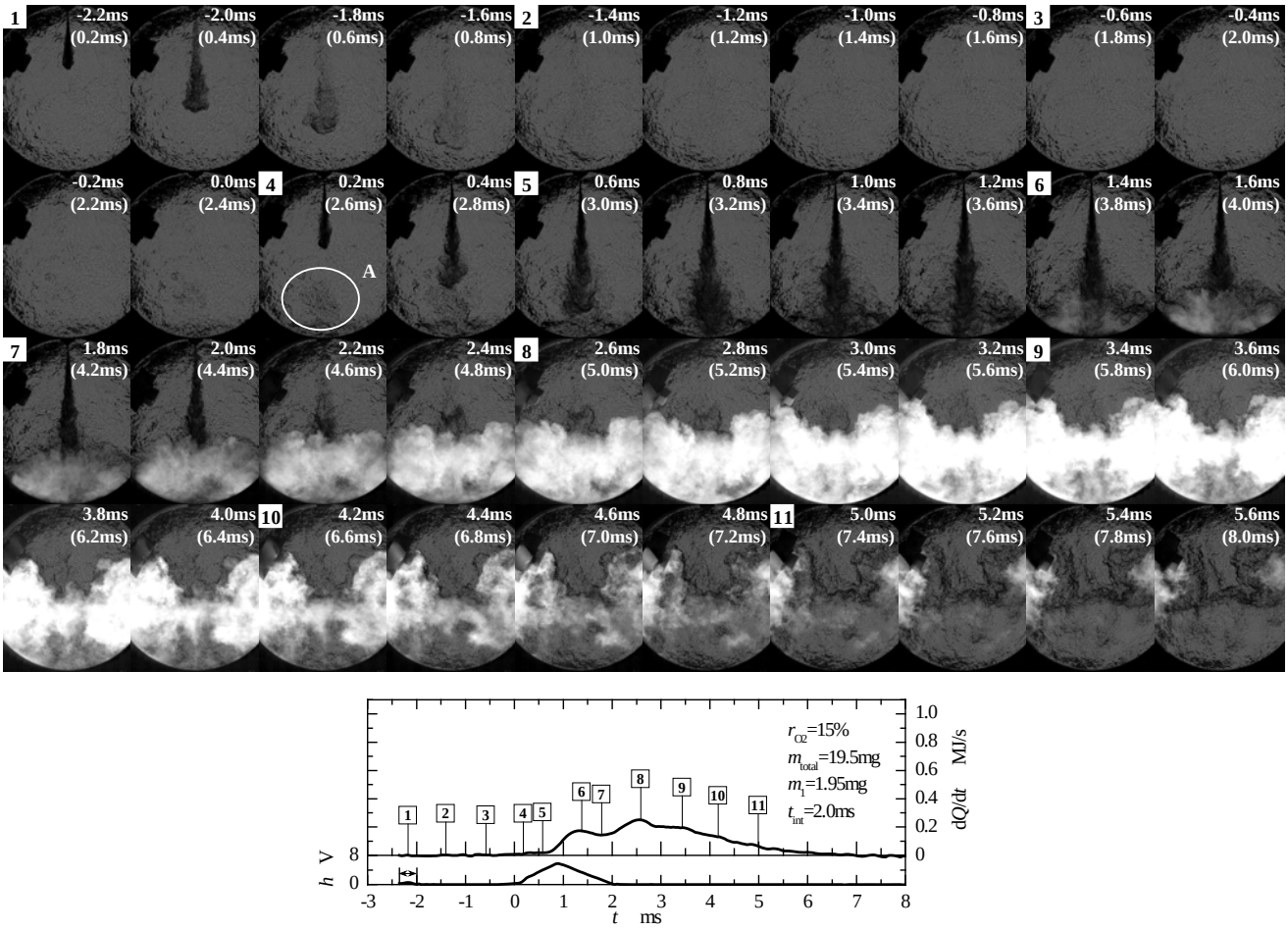

Fig. 21 Shadowgraph images and heat release rate (m_1 = 1.95 mg, t_{int} = 2.0 ms, r_{O2} = 15%)

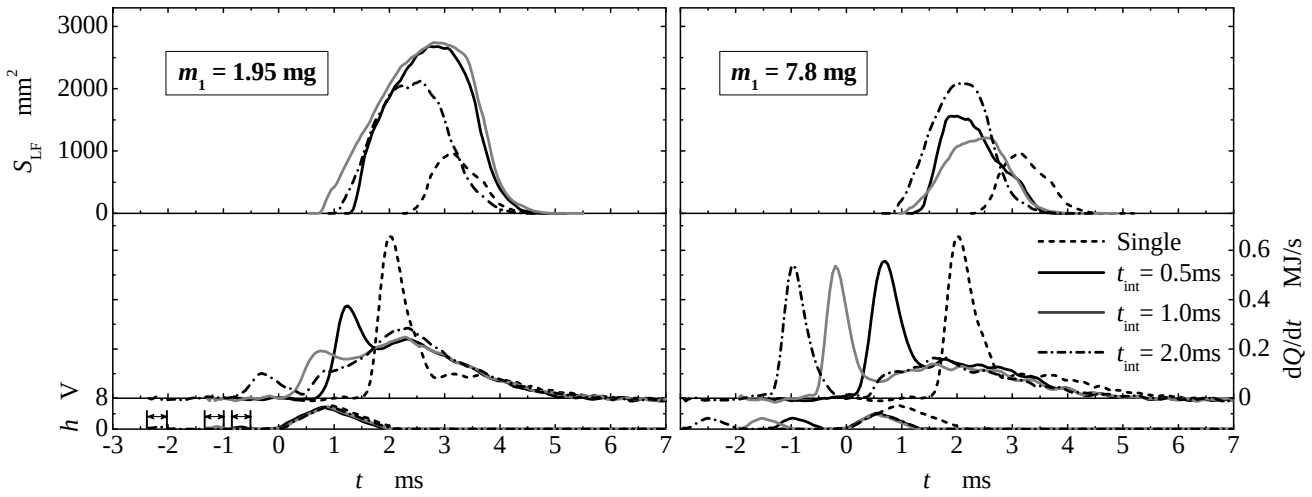

Fig. 22 Effects of injection dwell and fuel-quantity ratio on luminous-flame area and heat release rate (r_{O2} = 21%)

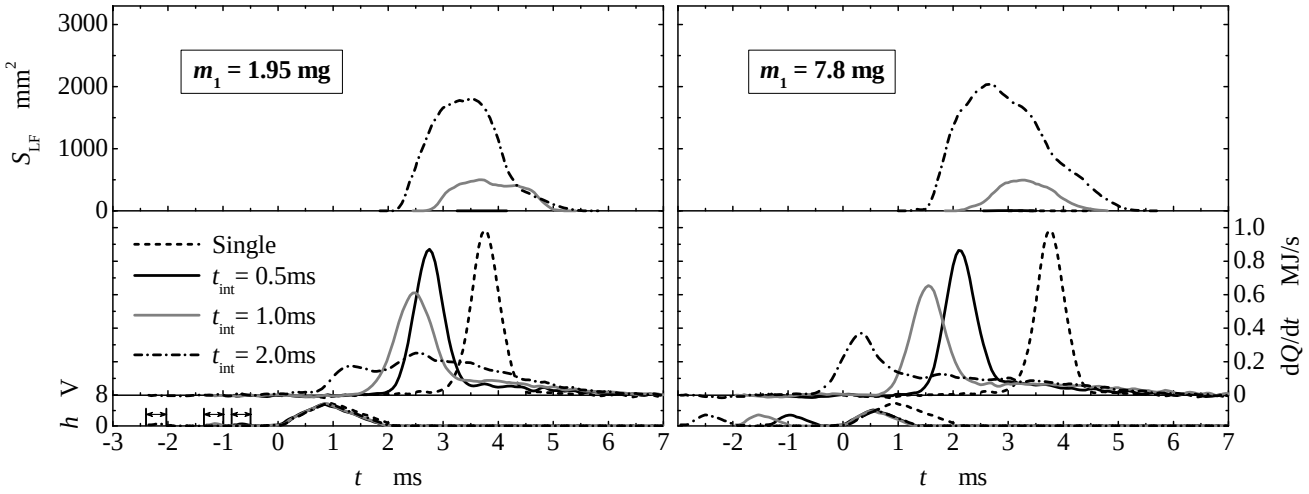

Fig. 23 Effects of injection dwell and fuel-quantity ratio on luminous-flame area and heat release rate (r_{O2} = 15%)

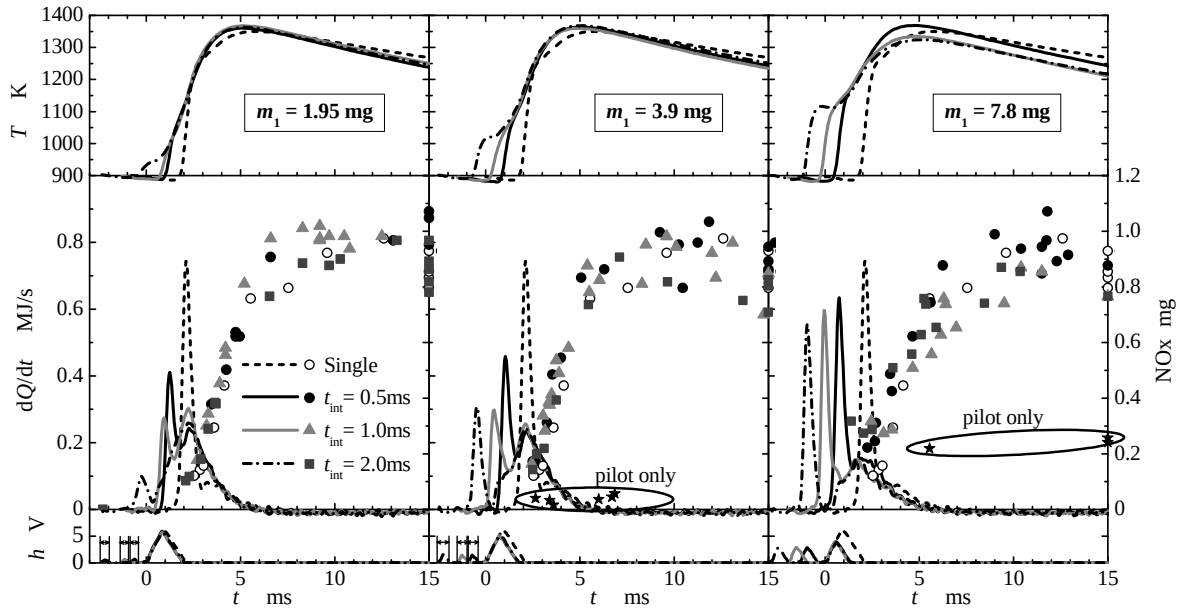

Fig. 24 Effects of injection dwell and first-injection quantity on NOx mass histories (r_{O2} = 21%)

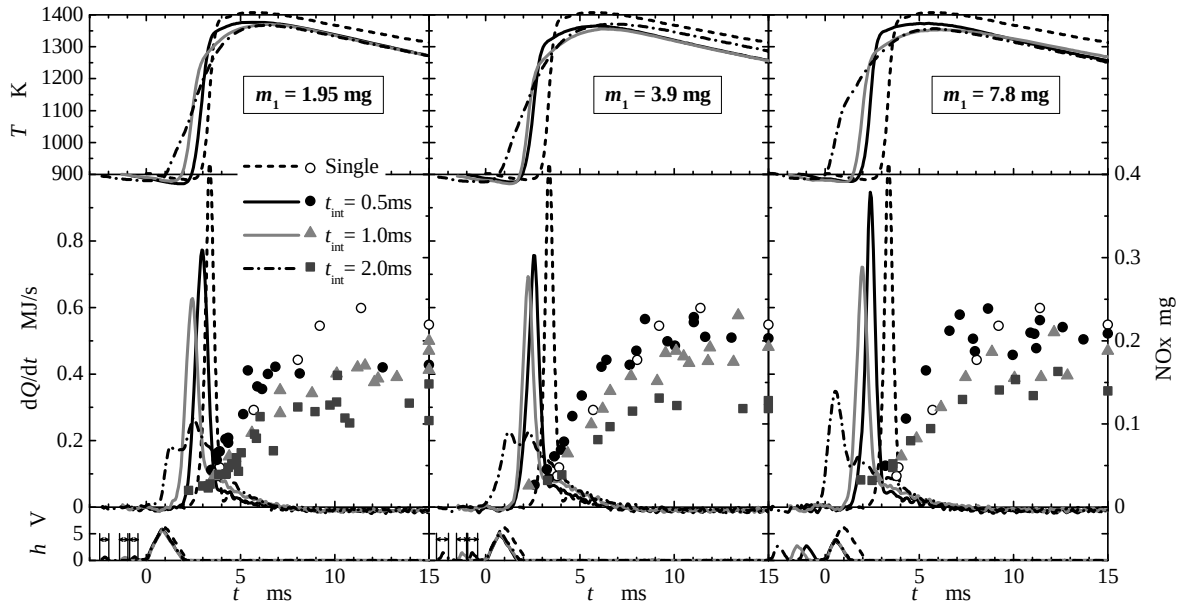

Fig. 25 Effects of injection dwell and first-injection quantity on NOx mass histories (r_{O2} = 15%)

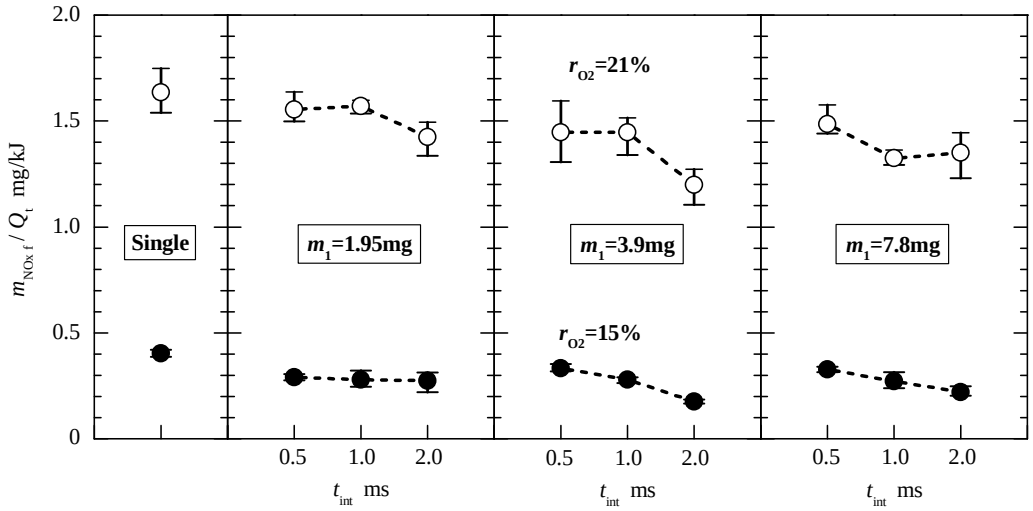

Fig. 26 Final NOx mass per heat release against injection dwell for various first-injection quantities